Excited State Protonation and Deprotonation Reactions of 6-Hydroxyquinoline Adsorbed in Y Zeolitic Supercages

Hyunung Yu, Hyojong Yoo, and Du-Jeon Jang*

Department of Chemistry and Research Institute of Molecular Science, Seoul National University, Seoul 151-742, Korea
Received September 24, 1996

Photon-initiated proton transfer cycles associated with excited and ground electronic states have been extensively studied for a variety of molecular systems.[1-6] However, proton transfer cycles involving excited states have been rarely studied using picosecond techniques in zeolites which show excellent catalytic effects, although the cycles have been reported in polymeric matrices[7] and in cyclodextrin cavities.[8] In this report picosecond time-resolved and static spectroscopic techniques are employed to study the protonation and deprotonation reactions of electronically excited 6-hydroxyquinoline (6HQN) introduced into catalytically important zeolitic cages.

Since one 6HQN molecule has two protropic functional groups, four protropic species of normal molecule (HQN), enol-deprotonated anion ($^-$QN), imine-protonated cation (HQNH$^+$), and enol-deprotonated and imine-protonated zwitterion ($^-$QNH$^+$) are equilibrated in aqueous solution (Scheme 1).[9] Hydroxyquinoline and their derivatives show very interesting aspects in both fundamental and practical points of view.[10-13] Drastically different effects of zeolites on encapsulated organic molecules from those of solvents have been studied by many groups,[14-16] since zeolites have well defined structures, cage effects and various unusual cationic interaction. Since acid and base sites of zeolites are believed to play important roles in zeolitic catalysis,[17] interactions of zeolitic acid and base sites with the enol and imine groups of 6HQN may exhibit interesting phenomena such as protropic equilibria, photon-induced proton transfers, cage effects, etc.. Our report will demonstrate that excited and ground state proton transfer cycles can be triggered by photons in organized zeolite media, and that a picosecond time-resolved fluorescence technique is a powerful tool for understanding the roles of acid and base sites in zeolitic catalysis.

6HQN was purchased from the Aldrich. Experimental procedures referring to materials and measurements were already reported in detail.[1,18] For kinetic measurements samples were excited only at 290 nm for the reason of limited laser availability.

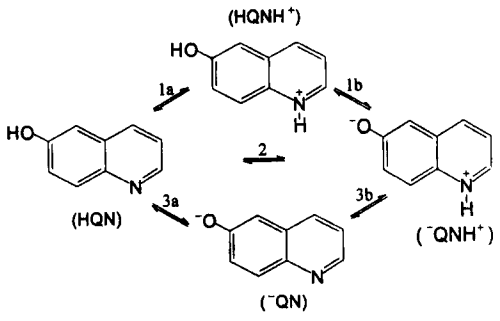

Scheme 1.

Both the diffuse reflectance and emission spectra of 6HQN adsorbed in supercages of Na$^+$-exchanged Y (NaY) zeolite, shown in Figure 1, are quite different from the absorption and emission spectra of aqueous 6HQN solutions, respectively, at any pH conditions. Although aqueous $^-$QNH$^+$ species is reported[9,13] to be unfavorable in both excited and ground states, the same species absorbing at 430 nm and fluorescencing at 510 nm is considerably favorable in zeolite cages, especially at the first excited singlet (S_1) state. The diffuse reflectance spectrum shows not only an enhanced absorption band of $^-$QNH$^+$ species but also absorption bands of all the other protropic species. This indicates that acid and base sites coexist at many different locations of the same zeolite and that NaY zeolite is heterogeneous at molecular level and more polar than water. The nearly neutral overall pH of NaY is owing to near equivalence in numbers of many strong acid and base sites, rather than the small numbers or weakness of both sites as expected in neutral solution systems.

Excitation at 325 nm, the peak absorption wavelength of HQN species, shows the emission spectrum predominant of $^-$QNH$^+$ emission. The large Stokes shift between the absorption and emission peaks suggests a consecutive photochemistry occurring at S_1 state. The fluorescence kinetic profiles of intrazeolitic 6HQN in Figure 2 verify this suggestion. As the collection wavelength of emission increases, both the formation and decay kinetics slow down. This as a whole indicates that the species emitting higher energy light sequentially transforms into the one emitting lower energy

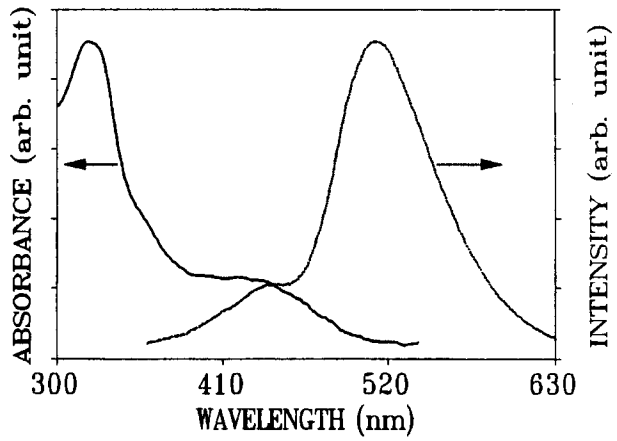

Figure 1. Diffuse reflectance (solid line) and emission (dotted line) spectra of 6HQN introduced into NaY supercages. The sample was excited at 325 nm for the emission spectrum.

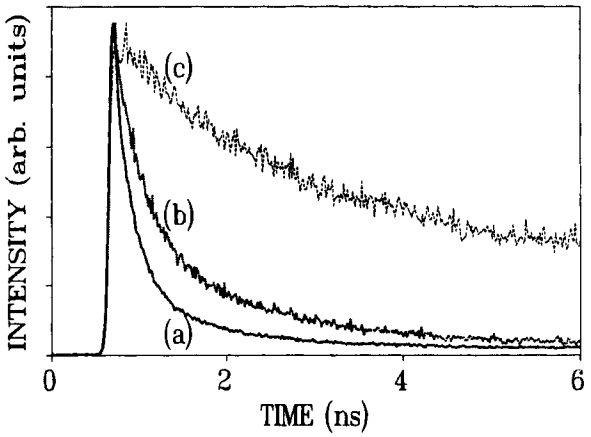

Figure 2. Fluorescence kinetic profiles of 6HQN adsorbed in NaY supercages. The sample was excited at 290 nm and the emission was collected at 370 (a), 430 (b) and 490 (c) nm. The deconvoluted time constants from these kinetic profiles are given in Table 1.

light in S_1. The fluorescence kinetic time constants given in Table 1 were deconvoluted from the kinetic profiles of Figure 2. The fluorescence decay kinetic time constants, rather than the fluorescence rise time constants, will be used to interpret the photochemical phenomena in S_1 since the rise kinetics contain more unavoidable errors than the decay kinetics by the following reasons. For instance, consider the kinetic profile of Figure 2(c) collected at 490 nm, the wavelength at which fluorescence from excited $^-QNH^+$ species is prevalent. Since a fluorescence spectrum usually has a long red tail, the kinetic profile at 490 nm includes the emission from excited HQN, ^-QN and $HQNH^+$ species. The primary reason for the faster formation at 490 nm than the decay at 430 nm is that the excitation of $^-QNH^+$ species existing at the ground state at the moment of excitation gives an instant rise.

The normal fluorescence kinetic profile at 370 nm in Figure 2(a) reveals three decay time constants as shown in Table 1. The 21 ps is ascribed to the protonation time of H-bonded imine group, the 180 ps to the protonation time of the imine group that has a proton nearby without H-bonding, and the 750 ps to the deprotonation time of the enol group of the HQN species that does not have any proton close to the imine group. These assignments are based on the following facts: (1) the imine-protonation is faster than the enol-deprotonation in aqueous solution. (2) the fastest component increases in proton-exchanged zeolite. (3) the slowest component increases in Na^+-exchanged X zeolite which has a higher basicity than NaY. (4) the employed NaY has many Brönsted-Lowry acid sites in spite of dehydration at 670 K but has exceedingly more Lewis base sites so that virtually every enol group is H-bonded to an oxygen atom of dehydrated zeolitic framework. Fluorescence at 430 nm is predominantly from the first excited singlet ^-QN and $HQNH^+$. The 320 ps from the profile at 430 nm is attributed to the imine-protonation time of the ^-QN species that has a proton close to its imine group without H-bonding and the 2200 ps to the enol-deprotonation time of $HQNH^+$ species. The 6500 ps at 490 nm is assigned to the

Table 1. Deconvoluted Fluorescence Kinetic Time Constants of 6HQN Intercalated into NaY Supercages[a]

Collection Wavelength[b] (nm)	Fluorescence Time Constant (ps)	
	Rise	Decay
370	Instant	21 (65%)[c]+180 (27%)+750 (8%)
430	25	320 (76%)+2200 (24%)
490	39	920 (31%)+6500 (69%)

[a] The molar ratio of 6HQN to the supercage was 0.5. [b] Samples were excited at 290 nm. [c] The percentages in parentheses are the relative amplitudes for the respective time constants.

relaxation time of excited $^-QNH^+$ species and the 920 ps to the observed overall time constant of cationic and anionic red tail fluorescence decay profiles since the collected wavelength is much shorter than 510 nm, the peak fluorescence wavelength of zwitterionic species.

Bardez *et al.*[13] have asserted that excited $^-QNH^+$ species in aqueous solutions transforms into a resonance hybrid structure of quinoid forms by intramolecular charge transfer within their temporal resolution, emitting at much a longer wavelength. However, fluorescence kinetic profiles as well as diffuse reflectance and emission spectra apparently show that the subsequent electron rearrangement following the formation of excited $^-QNH^+$ species does not occur in NaY supercages. Complete data, thorough analyses and detailed interpretation will be reported in a later full article. However, this brief report makes evident that protropic photocycles can be drived in catalytically important zeolitic cages and introduces a new time-resolved approach to comprehend the catalytic functions of acid and base sites in zeolites.

Acknowledgment. We thank Dr. Dongho Kim and Dr. Nam Woong Song at the Korea Research Institute of Standards and Science for measuring kinetic profiles. This work was financially supported by the Hallym Academy of Sciences, Hallym University and the Korea Ministry of Education.

References

*Also a member of the Center for Molecular Science, Taejon 305-701, Korea.

1. Lee, S.-I.; Jang, D.-J. *J. Phys. Chem.* **1995**, *99*, 7537.
2. Roberts, E. L.; Chou, P. T.; Alexander, T. A.; Agbaria, R. A.; Warner, I. M. *J. Phys. Chem.* **1995**, *99*, 5431.
3. Chudoba, C.; Lutgen, S.; Jentzsch, T.; Riedle, E.; Woerner, M.; Elsaesser, T. *Chem. Phys. Lett.* **1995**, *240*, 35.
4. Syage, J. A. *J. Phys. Chem.* **1995**, *99*, 5772.
5. Parsapour, F.; Kelley, D. F. *J. Phys. Chem.* **1996**, *100*, 2791.
6. Logunov, S. L.; El-Sayed, M. A.; Song. L.; Lanyi, J. K. *J. Phys. Chem.* **1996**, *100*, 2391.
7. Douhal, A.; Dabrio, J.; Sastre, R. *J. Phys. Chem.* **1996**, *100*, 149.
8. Park, H.-R.; Mayer, B.; Wolschann, P.; Köhler, G. *J. Phys. Chem.* **1994**, *98*, 6158.
9. Mason, S. F.; Philp, J.; Smith, B. E. *J. Chem. Soc. (A)* **1968**, 3051.
10. Matsumura, M.; Akai, T.; Saito, M.; Kimura, T. *J. Appl.*

Phys. **1996**, *79*, 264.
11. Kim, T.-G.; Lee, S.-I.; Jang, D.-J.; Kim, Y. *J. Phys. Chem.* **1995**, *99*, 12698.
12. Nakagawa, T.; Kohtani, S.; Itoh, M. *J. Am. Chem. Soc.* **1995**, *117*, 7952.
13. Bardez, E.; Chatelain, A.; Larrey, B.; Valeur, B. *J. Phys. Chem.* **1994**, *98*, 2357.
14. Park, J.; Kang, W.-K.; Ryoo, R.; Jung, K.-H.; Jang, D.-J. *J. Photochem. Photobiol. A: Chem.* **1994**, *80*, 333.
15. Ehrl, M.; Kindervater, H. W.; Deeg, F. W.; Bräuchle, C.; Hoppe, R. *J. Phys. Chem.* **1994**, *98*, 11756.
16. Florián, J.; Kubelková, L. *J. Phys. Chem.* **1994**, *98*, 8734.
17. Bhatia, S. *Zeolite Catalysis: Principles and Applications*; CRC Press: Boca Raton, Florida, 1990; p 75.
18. Kang, W.-K.; Cho, S.-J.; Lee, M.; Kim, D.-H.; Ryoo, R.; Jung, K.-H.; Jang, D.-J. *Bull. Korean Chem. Soc.* **1992**, *13*, 140.

Highly Regioselective Electrochemical Epoxide Ring Opening Reactions by Alkyl Halides Using Sacrificial Anodes and Stainless Steel Cathode

Jung Hoon Choi*, Jeong Su Kim, Jong sung Youm, Book Kee Hwang, Tae Kee Hong†, and Choong Eui Song‡

Department of Chemistry, Hanyang University, Seoul 133-791, Korea
†Department of Chemistry, Hanseo University, 360, Daegokri, Haemi, Seosan, Chung-Nam, 352-820, Korea
‡Korea Institute of Science and Technology, P.O. box 131, Cheongryang, Seoul 130-650, Korea
Received October 1, 1996

Electrochemical technique has been known as a powerful tool in generating many active species which may not be formed by conventional chemical methods. As a matter of fact, a wide variety of organic chemical transformations can be carried out rapidly and in good yields, using relatively simple equipment, with the added advantage of avoiding harzardous, toxic reagent or byproduct. Especially, electrochemical process by a sacrificial anode in order to permit the formation of carbanions in undivided cell provided an extremely convenient methodology. That is, normally carbanions generated at the cathode would migrate to the anode and be destroyed by oxidation there. However, if the anode is made of an electropositive metal, the anode reaction becomes oxidation of the metal anode itself. These metal ions formed at the anode presumably coordinate with the carbanions generated electrochemically at the cathode to afford organometallic species, which react more readily with added electrophile than the free carbanion. In order to apply this view to the synthetic purposes, we decided to utilize this sacrificial anode for electrochemical epoxide ring opening reactions by alkyl halides. The electrochemical results of our study are summarized in Table 1 along with comparative data for Grignard reactions of the corresponding epoxides.

In our electrochemical epoxide ring opening reactions with alkyl halides, stainless steel as working electrode, and copper, magnesium, aluminium and zinc as sacrificial anodes were employed. And tetrabutylammonium tetrafluoroborate ($TBABF_4$) as a supporting electrolyte and N,N-dimethylformamide (DMF) as a solvent were used in these electrochemical reactions. The amount of epoxide ring opening products was measured as current yields which were the ratio of the actual amount consumed to theoretical amount of electricity required to effect a given reaction. And regioselectivity of electrochemical reaction products was compared with Grignard reaction products.

As would be anticipated for an S_N2 process, electrochemical epoxide ring opening occurs at the less substituted position. In the case of 1,2-epoxybutane with primary alkyl halide, such as 1-bromobutane, current yields were quite different to depend upon the sacrificial anodes but the regioselectivity of products was very high compared to those of Grignard reactions. Furthermore, as the alkyl halides become more bulkier, the regioselectivity was increased dramatically in electrochemical processes. Especially in the case of tertiary alkyl halide such as 2-bromo-2-methylpropane, the regioselectivity was shown to be 100%. It was very suprising results compared with Grignard reaction which gave the corresponding products in a ratio of 89 : 11. However, the electrochemical reaction of benzylchloride with 1,2-epoxybutane afforded the low regioselectivity like Grignard reaction. In the case of styrene oxide with alkyl halides, all electrochemical reactions gave the sole product in a ratio of 100 : 0 while Grignard reaction afforded the two products in considerably low regioselectivity.

Although we do not have the reasonable explanation for these high regioselectivities of this electrochemical epoxide ring opening reactions, we could explain as follows. First of all, metal cations are generated at the sacrificial anode, and coodinate to the electron rich site of epoxides. These epoxides, being positively charged by metal cation, will move toward the cathode. At the same time, the carbanions are generated by the alkyl halides on the cathode surface. And these two charged species are arranged in order of carbanions and epoxides on the bulky cathode suface to have the less steric hindrance each other, and they react rapidly before they are diffused uniformly into the solution as shown in Scheme 1.